https://doi.org/10.5194/egusphere-2026-5486
Preprint. Discussion started: 22 September 2026

How the North Atlantic storm track builds the moisture supply to warm conveyor belt ascent

Marc Federer[1] and Talia Tamarin-Brodsky[1]

[1]Department of Earth, Atmospheric and Planetary Sciences, Massachusetts Institute of Technology, Cambridge, MA, USA

Correspondence: Marc Federer (mfederer@mit.edu)

Abstract. The moisture entering warm conveyor belt (WCB) ascent constrains the latent heat release that shapes extratropical cyclone development and the downstream circulation, yet the processes establishing this moisture remain poorly studied. Using 10-day backward trajectories initialized from North Atlantic WCB inflows in ERA5 over 43 winters (1980–2022), we identify four main dynamical histories of the inflowing air based on which environments shaped their moisture pick-up: cold air outbreak (CAO), fast descent, slow descent, and subtropical origin. WCB inflow is a superposition of these pathways, whose moisture is predominantly of recent extratropical origin and is acquired on strongly pathway-dependent timescales, ranging from about two days for the CAO and fast descent pathways to four to six days for air of subtropical and slow descent origin. We then ask why some WCBs are anomalously moist, while others remain relatively dry. We find that moist and dry inflows differ markedly in pathway composition, with subtropical origin air replacing CAO air for anomalously moist WCBs, but this shift contributes little to the moisture anomaly because the opposing compositional changes nearly cancel. The anomaly instead arises within the pathways: air arriving through every pathway is itself anomalously moist. Within each pathway, moist and dry inflows undergo similar thermodynamic evolution, but moist inflows progress farther toward warmer and more saturated conditions before ascent, while dry inflows are incorporated into the WCB at an earlier stage of this evolution. This difference is established well before WCB inflow: air feeding moist WCBs takes up moisture earlier, after an extended equatorward excursion on the flank of an antecedent anticyclone, whereas air feeding dry WCBs is moistened within a recent CAO shortly before ascent. The two groups are nonetheless embedded in nearly identical sea level pressure patterns at inflow, so their contrasting moisture is not apparent from the circulation at the onset of WCB ascent. How moist a WCB inflow becomes is therefore not determined by pathway identity alone, but by the preconditioning accumulated along that pathway. The antecedent circulation shapes both the route taken toward WCB ascent and how far air progresses along its associated thermodynamic evolution, thereby preconditioning the moisture available for latent heat release during WCB ascent.

1 Introduction

Moisture plays a central role in the dynamics of extratropical weather systems (Wernli and Gray, 2024). Latent heat release can intensify extratropical cyclones (Ahmadi-Givi et al., 2004; Binder et al., 2016; Federer et al., 2024), amplify and maintain upper-level ridges and blocking anticyclones (Pfahl et al., 2015; Steinfeld and Pfahl, 2019; Wenta et al., 2024), influence high-impact weather downstream (Grams et al., 2011), and shape the midlatitude storm tracks (Hoskins and Valdes, 1990;

https://doi.org/10.5194/egusphere-2026-5486
Preprint. Discussion started: 22 September 2026

Tamarin-Brodsky and Kaspi, 2017; Schemm, 2023). Much of this heating occurs within warm conveyor belts (WCBs), the coherent airstreams that ascend rapidly from the lower into the upper troposphere within extratropical cyclones (Wernli and Davies, 1997; Madonna et al., 2014; Heitmann et al., 2024; Hwang et al., 2026). The moisture entering this ascent sets an important thermodynamic boundary condition on the diabatic evolution of the WCB: it limits how much water can condense, how much latent heat can be released, and thus how strongly the ascending air can potentially modify the large-scale circulation (Martínez-Alvarado et al., 2014; Schäfler and Harnisch, 2015). Yet this inflow moisture is itself organized by the storm track. Over the preceding days, the inflow air can descend, interact with the ocean surface, take up moisture repeatedly, and travel large distances within the evolving storm track. Understanding the diabatic influence of WCBs therefore also requires understanding how the atmosphere builds the moisture reservoir on which WCB ascent feeds.

One important source of this reservoir is evaporation within the extratropical storm track itself. Most WCB inflow moisture is acquired within the midlatitudes, predominantly during the final five days before ascent (Pfahl et al., 2014). Wintertime ocean evaporation is highly intermittent and becomes strong when cold or dry air is brought into contact with warmer water (Aemisegger and Papritz, 2018). It is most prominent during cold air outbreaks (CAOs), when cold polar or continental air is advected over a relatively warm ocean, generating large air–sea contrasts and strong surface fluxes (Grossman and Betts, 1990; Papritz et al., 2015; Papritz and Spengler, 2017). CAOs occur frequently in cyclone cold sectors, especially downstream of the western boundary currents, and rapidly warm and moisten initially cold and dry air (Schultz et al., 1998; Walsh et al., 2001; Schnyder and Riboldi, 2026). A related pathway involves dry air descending from the free troposphere within dry intrusions (DIs) behind the cold front of cyclones (Raveh-Rubin, 2017; Catto and Raveh-Rubin, 2019). Where this dry air reaches the marine boundary layer, the large humidity deficit drives strong uptake from the ocean. Both CAOs and DIs therefore tie the moisture supply to the storm track circulation, which creates and transports the cold and dry air masses that subsequently undergo strong air–sea interaction.

The air moistened in the cold sector of one cyclone need not ascend within that same system. Several studies have identified a moisture handover between successive cyclones, in which air is moistened in the cold sector of a cyclone before entering the warm sector of a later system, where it eventually ascends (Sodemann and Stohl, 2013; Papritz et al., 2021; Demirdjian et al., 2023). Dacre et al. (2019) describe this low-level supply as a feeder airstream: a moist, rearward cyclone-relative flow through the warm sector that feeds the base of the WCB. This handover connects air–sea interaction associated with one system to latent heating within a subsequent one (Wenta et al., 2024; Quinting et al., 2026), so that WCB inflow moisture can retain a memory of storm track evolution over several days.

A complementary perspective emphasizes moisture supplied from lower latitudes. In the zonal mean, ocean evaporation peaks in the subtropics, while the circulation transports water vapor poleward into the midlatitudes (Peixoto et al., 1992; Walker and Schneider, 2006; Pauluis et al., 2008). On synoptic scales, this transport appears as tropical moisture exports (TMEs), elongated bands of moist air reaching from the subtropics into the extratropics (Knippertz and Wernli, 2010; Knippertz et al., 2013). Atmospheric rivers (ARs) similarly identify narrow corridors that accomplish much of the poleward vapor transport and are closely tied to heavy coastal precipitation (Newell et al., 1992; Ralph et al., 2006; Guan and Waliser, 2015). Strong poleward transport does not, however, uniquely identify the origin of the transported vapor. Lagrangian analyses show that

https://doi.org/10.5194/egusphere-2026-5486
Preprint. Discussion started: 22 September 2026

a substantial fraction of AR moisture is acquired recently within the midlatitudes through convergence of locally moistened feeder air, rather than through direct transport from the tropics (Sodemann and Stohl, 2013; Dacre et al., 2015). The local and remote perspectives are therefore not mutually exclusive: a single WCB inflow can combine recently transformed extratropical air with air of prolonged subtropical origin.

Together, these studies point to a broader open question in moist storm track dynamics. Much is known about how latent heat release modifies a cyclone and its downstream circulation once moist ascent occurs, but less about how the thermodynamic state entering that ascent is established, and how prominent events like CAOs, DIs and TMEs contribute. Storm track eddies continually redistribute, descend, moisten, and recirculate air, thereby shaping the environment encountered by later weather systems. Air entering WCB ascent may experience a wide range of dynamical and thermodynamic conditions before reaching the cyclone. These different histories can shape where, when, and under which conditions moisture is acquired. Understanding WCB moisture supply therefore requires tracing the evolution of the inflowing air before it enters the WCB and identifying which aspects of that history establish its thermodynamic state at inflow.

This antecedent evolution also has implications for predictability. WCBs are known to amplify forecast errors in the midlatitudes through their interaction with upper-level Rossby waves (Rodwell et al., 2013; Oertel et al., 2020; Sánchez et al., 2020; Pickl et al., 2023). An important source of these errors is the imperfect representation of latent heat release during WCB ascent in numerical weather prediction models (Lojko et al., 2025; Rixen et al., 2026). Yet errors can arise before the ascent itself: biases in the moisture content and transport of WCB inflow can rapidly amplify, affecting subsequent cyclone development and the downstream circulation (Schäfler and Harnisch, 2015; Christ et al., 2025; Yu et al., 2025). The processes controlling this antecedent source of error remain less systematically understood. Identifying the pathways that feed WCB ascent and the timescales over which they acquire moisture therefore constrains an important part of this error chain: the processes that establish the moisture available for subsequent diabatic heating. In this way, the pathway perspective connects the antecedent evolution of the storm track to the diabatic processes shaping subsequent cyclone development and the downstream flow.

Here we investigate how the North Atlantic storm track constructs the moisture supply to WCB ascent, using 10-day backward trajectories initialized from WCB inflows in ERA5 during Northern Hemisphere winter (DJF) 1980–2022. We classify inflow air into four dynamical and thermodynamic histories—CAO, fast descent, slow descent, and subtropical origin—and address two questions:

(Q1) How is WCB inflow moisture assembled from different dynamical and thermodynamic histories, and over what timescales is that moisture acquired?

(Q2) What distinguishes anomalously moist from dry WCB inflows, and when in their antecedent evolution is that difference established?

Section 2 describes the data and trajectory methodology. Section 3 addresses Q1 by introducing the pathway classification and quantifying the associated thermodynamic histories, moisture contributions, and uptake timescales. Section 4 addresses Q2 by decomposing the humidity difference between anomalously moist and dry WCBs into changes in pathway composition and changes in moisture content within each pathway, and by examining their antecedent uptake, thermodynamic evolution, and

https://doi.org/10.5194/egusphere-2026-5486
Preprint. Discussion started: 22 September 2026

synoptic setting. As will be shown, WCB inflow is a superposition of air masses with strongly contrasting upstream histories, yet these histories do not uniquely determine how moist the inflow becomes. Instead, provenance primarily sets the route and timescale by which moisture reaches the WCB, while the amount ultimately delivered depends on how the circulation preconditions the air along that route before ascent. The moisture entering a WCB therefore retains a memory of the preceding evolution of the storm track, not only through where its air comes from, but through the dynamical history that establishes its thermodynamic state before ascent.

2 Data and methods

2.1 Reanalysis data

The analysis is based on the ERA5 reanalysis (Hersbach et al., 2020) for the 42 December–January–February (DJF) periods in 1980–2022. Fields are interpolated to a horizontal resolution of $0.5° \times 0.5°$ at hourly temporal resolution, on the native ERA5 hybrid sigma–pressure model levels (137 levels). We use instantaneous fields of wind, temperature, specific humidity, and pressure, as well as surface fields and accumulated quantities, including large-scale and convective precipitation.

The CAO index used in the trajectory classification is computed hourly on the ERA5 grid as the difference between SST and potential temperature at 850 hPa, $\mathrm{CAO} = \mathrm{SST} - \theta_{850}$, following Papritz and Spengler (2017). A CAO is identified if the CAO index exceeds 4 K.

2.2 WCB trajectories

WCB trajectories are taken from the ERA5-based WCB climatology of Heitmann et al. (2024), which was calculated using the Lagrangian analysis tool LAGRANTO (Wernli and Davies, 1997; Sprenger and Wernli, 2015). In this climatology, trajectories are initialized every 6 h on an approximately equidistant 80 km grid and at 20 hPa intervals between 790 and 1050 hPa, and are classified as WCB trajectories if they ascend by at least 600 hPa within a 48 h period. The required pressure decrease can occur at any time within this interval, thereby also including rapidly ascending trajectories that subsequently descend. WCB trajectories are grouped into coherent bundles when their starting positions lie within 250 km of at least one other WCB trajectory. A bundle is retained if at least one of its constituent trajectories intersects an extratropical cyclone mask during the 48 h ascent, and all trajectories belonging to such a bundle are included irrespective of whether each individual trajectory intersects the cyclone mask. A double-counting filter removes trajectories that satisfy the WCB criteria at multiple initialization times. Cyclones are identified from sea-level pressure contours following Wernli and Schwierz (2006) and Sprenger et al. (2017).

To investigate the air parcel history prior to WCB ascent, we follow the methodology presented in Pfahl et al. (2014). We extend each identified WCB trajectory backward from its starting position by calculating a 10-day backward trajectory with LAGRANTO using ERA5 wind fields. These backward trajectories retain the bundle assignment of the corresponding WCB trajectories, allowing the pre-ascent evolution of individual air parcels to be related to the coherent WCB into which they

https://doi.org/10.5194/egusphere-2026-5486
Preprint. Discussion started: 22 September 2026

are subsequently incorporated. All analyses of WCB inflow origin, thermodynamic evolution, and moisture uptake presented here are based on these 10-day backward extensions, while WCB identification and bundle membership are inherited from the original WCB climatology. For our North Atlantic analysis, we consider WCB trajectories with inflow locations within the domain $100°$W–$40°$E and $15°$N–$75°$N.

2.3 Moisture source diagnostic

We diagnose when and where the moisture present at WCB inflow was acquired using the established Lagrangian moisture source attribution framework of Sodemann et al. (2008), following its implementation for hourly ERA5 trajectories by Papritz et al. (2021). The WCB inflow time is defined as $t = 0$, with negative times denoting the preceding air parcel history. Hourly increases in specific humidity along a trajectory are interpreted as moisture uptake, whereas decreases represent moisture loss. Following Papritz et al. (2021), only increases exceeding $0.025\,\mathrm{g\,kg^{-1}\,h^{-1}}$ are retained as uptake events, thereby excluding numerical noise and small fluctuations in specific humidity.

To account for moisture acquired at an earlier time that is subsequently lost before WCB inflow, the identified uptake events are corrected for subsequent moisture losses following Sodemann et al. (2008). The trajectory is evaluated chronologically from the beginning of the 10-day period toward WCB inflow, and at each moisture-loss event all preceding moisture contributions are reduced by the same fractional amount as the parcel's specific humidity. Specifically, if specific humidity decreases from q_{t-1} to q_t, each preceding moisture contribution is multiplied by q_t/q_{t-1}. This correction is applied iteratively to all moisture losses between each uptake event and WCB inflow. The resulting attributed uptake, $\mathrm{d}q(t)$, therefore represents the portion of moisture acquired at time t that remains in the parcel at WCB inflow. An illustrative example of this established attribution procedure is provided in Appendix A and Fig. A1.

We express each attributed uptake as a fraction of the parcel specific humidity at inflow, $f(t) = \mathrm{d}q(t)/q(t=0)$. The cumulative contribution $f_{\mathrm{tot}}(t)$ is the fraction of inflow moisture attributed to uptake between time t and WCB inflow. Consequently, $1 - f_{\mathrm{tot}}(t)$ represents moisture that cannot be attributed to resolved uptake events during this interval. This unresolved contribution consists of moisture already present when the trajectory is initialized together with contributions from moisture increases below the uptake threshold.

Finally, we identify the dominant moisture uptake period of each trajectory from the centered 12-h running sum of $\mathrm{d}q$. The time of the largest 12-h accumulated uptake is denoted $t_{\max}$ and used as the Lagrangian reference time of the dominant moisture source event.

3 WCB inflow is a superposition of thermodynamically distinct pathways

3.1 A case example

We begin with a case study of a single WCB inflow, which illustrates several characteristics that we subsequently generalize climatologically. This inflow occurred at 00 UTC on 20 February 2022.

https://doi.org/10.5194/egusphere-2026-5486
Preprint. Discussion started: 22 September 2026

Figure 1 shows the air parcel trajectories and the surrounding synoptic flow at three stages leading up to the inflow and the eventual ascent of the WCB. Five days (120 h) before the inflow, a large cluster of parcels lies on the subtropical flank of a high pressure system (H) (Fig. 1a), having traveled westward within the trade wind region of the lower troposphere over the preceding three days. A second, extratropical cluster is present at the same time along the eastern seaboard of North America, embedded in the cold air advection behind a surface cyclone (L1). Some of these parcels have already reached the lower troposphere while others are still descending from the middle troposphere, and their paths trace back to the Arctic. Two coherent clusters, one subtropical and one extratropical, are thus present well before the associated cyclone and its WCB develop.

Sixty hours later, the subtropical cluster has progressed farther west and the extratropical cluster farther southeast (Fig. 1b). On the subtropical flank of a high pressure system (H), the two clusters merge into a single, coherent airstream that circulates anticyclonically and forms the feeder airstream of the cyclone that subsequently develops (L2). By the inflow time, the parcels have completed this circuit, wrapping around the western edge of the high as it migrates eastward and feeding the warm sector of the developing cyclone (L2) (Fig. 1c). As the cyclone moves through the North Atlantic, the air parcels ascend into the upper troposphere as a coherent WCB (Fig. 1d).

The case study foreshadows two features that recur throughout the analysis. First, WCB inflow air is typically of mixed origin, drawing on both subtropical and extratropical histories rather than on a single source. Second, these histories converge on the subtropical flank of a high pressure system to form the cyclone's feeder airstream, which, viewed over the full trajectories, appears as an anticyclonic recirculation into the inflow. The following sections will systematically characterize the thermodynamic and dynamic differences between the pathways and assess how strongly a parcel's history controls the moisture reaching the inflow.

3.2 WCB inflow trajectory classification

The goal of this classification is to systematically distinguish the air streams feeding WCBs according to their characteristic moistening pathways. The classification is designed to be exhaustive and mutually exclusive, such that each WCB inflow trajectory is assigned to exactly one category. Aemisegger et al. (2021) investigated the role of Rossby wave breaking in the hydrological cycle of the trade-wind region using a classification based primarily on the magnitude of air parcel descent. We adapt this framework to the midlatitude storm tracks by additionally accounting for moisture uptake during CAOs over the western boundary currents and for the poleward transport of air masses of subtropical origin. The resulting classification distinguishes between the import of moisture from lower latitudes and different dynamical pathways leading to moisture uptake within the extratropics.

We adopt a hierarchical classification. We first identify trajectories of subtropical origin, which are intended to capture tropical moisture exports. A trajectory is classified as subtropical if it resides equatorward of 30°N for at least 70% of the period from 8 to 3 days prior to WCB inflow. Since most WCB inflow occurs poleward of 30°N, the residence criterion excludes the final three days before inflow to allow for poleward transport into the cyclone. The 70% residence threshold reduces sensitivity to trajectories that repeatedly cross the 30°N boundary.

https://doi.org/10.5194/egusphere-2026-5486
Preprint. Discussion started: 22 September 2026

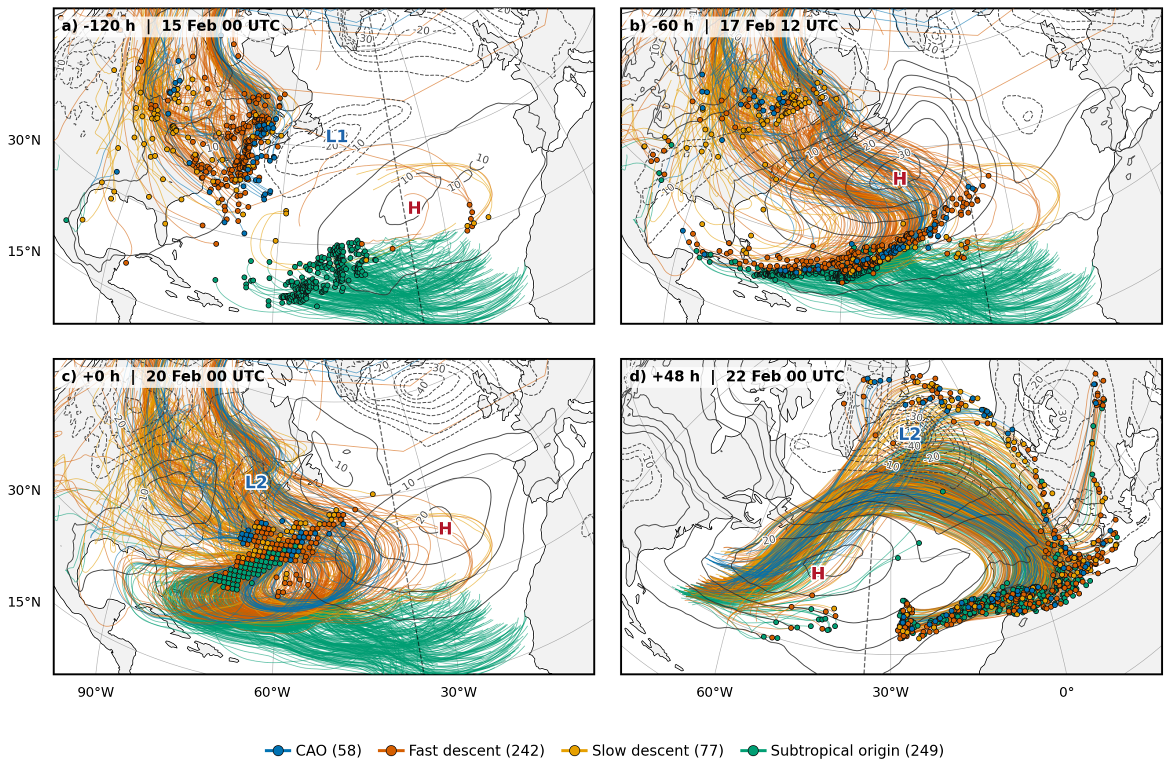

Figure 1. Case study of a WCB inflow on 20 Feb 2022, 00 UTC. Mean sea-level pressure anomalies (grey contours) and instantaneous trajectory locations (colored dots) are shown for (a) 15 Feb 2022, 00 UTC, (b) 17 Feb 2022, 12 UTC, (c) 20 Feb 2022, 00 UTC and (d) 22 Feb 2022, 00 UTC. The path of the backward trajectories in panels (a)-(c) are shown between 8 days before they arrive in the WCB inflow and the respective time step, and are colored by pathway. Panel (d) shows the 48-h forward trajectories ascending from the WCB inflow. At inflow (c), several dots are stacked vertically, and the color represents the majority classification on that initialization point. ’L’ and ’H’ mark low- and high-pressure systems, respectively, which are discussed in the text.

All remaining trajectories are classified as extratropical in origin. These categories are defined relative to the time of maximum moisture uptake. Trajectories located within a CAO at the time of maximum moisture uptake are assigned to the *CAO* category, representing moisture uptake associated with strong air–sea temperature contrasts. The remaining trajectories are separated according to their vertical displacement during the four days preceding maximum moisture uptake. Trajectories descending by more than 100 hPa are classified as *fast descent*, representing moisture uptake associated with strong relative humidity gradients, analogous to dry intrusions descending into the boundary layer. Trajectories descending by less than 100 hPa are classified as *slow descent*, which serves as the residual extratropical category. The threshold of 100 hPa corresponds approximately to the radiative descent of an air parcel in the free troposphere without dynamical forcing (Aemisegger et al., 2021). The different pathways, and their mean moisture contribution to North Atlantic WCBs, are summarized in Table 1.

https://doi.org/10.5194/egusphere-2026-5486
Preprint. Discussion started: 22 September 2026

Table 1. Summary of the WCB inflow classification. Mean moisture contributions and specific humidity at WCB inflow for North Atlantic WCBs.

Category	**Origin**	**Definition**	**Contribution (%)**	$\overline{q}_{\text{inflow}}$ (g kg^{-1})
Subtropical	Subtropical	$>$ 70% residence south of 30°N (8–3 d before inflow)	29	10.3
CAO	Extratropical	Maximum moisture uptake within a CAO	20	8.1
Fast descent	Extratropical	$>$ 100 hPa descent during the 4 d before max. moisture uptake	37	8.7
Slow descent	Extratropical	$<$ 100 hPa descent during the 4 d before max. moisture uptake	14	8.7

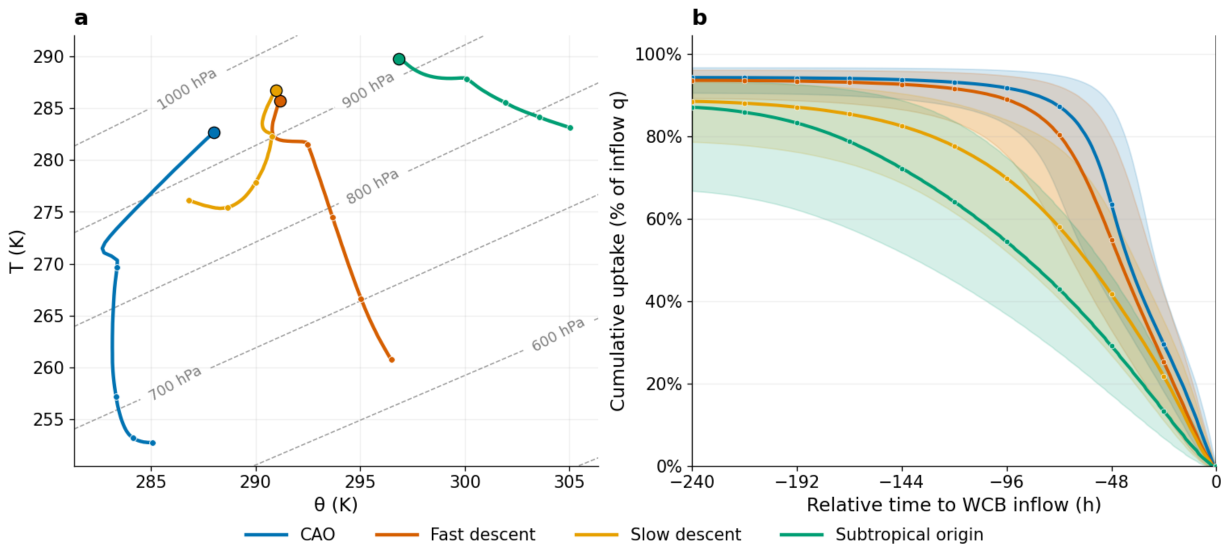

Figure 2. (a) Thermodynamic $\theta - T$ diagram showing the median thermodynamic evolution of the four WCB inflow pathways from the time of maximum moisture pick up (big dot) backward in time. Small dots indicate 24 h intervals. (b) Median cumulative percentage of the moisture present at WCB inflow ($t = 0$) acquired along the trajectories up to each backward time for the four pathways. Shading denotes the interquartile range (25th–75th percentiles).

3.3 Thermodynamic histories and moisture-uptake timescales

Figure 2 illustrates the thermodynamic evolution and moisture-uptake timescales of the four pathways. Figure 2a shows their median thermodynamic evolution prior to maximum moisture uptake in the phase space of potential and absolute temperature. Maximum moisture uptake occurs below 900 hPa for all pathways, although the subtropical pathway reaches this level at substantially higher temperatures than the extratropical pathways.

Before maximum moisture uptake, subtropical air parcels undergo radiative cooling, as indicated by decreasing potential temperature. At the same time, the parcels descend, and adiabatic compression more than compensates for the diabatic cooling, resulting in a slight increase in absolute temperature.

https://doi.org/10.5194/egusphere-2026-5486
Preprint. Discussion started: 22 September 2026

The extratropical pathways exhibit fundamentally different behavior. CAO air parcels descend nearly adiabatically until reaching the boundary layer, where they undergo rapid diabatic warming. Fast descent air parcels begin their descent from a warmer environment, descend more rapidly than CAO parcels, and experience weaker diabatic warming near the surface. In contrast, slow descent air parcels originate on average below 800hPa and undergo gradual diabatic warming before converging with the fast descent pathway near 900hPa.

All four pathways exhibit a brief but pronounced cooling around 850 hPa. We hypothesize that this feature is associated with cloud processes, potentially through radiative cooling or evaporative cooling near cloud top.

The distinct thermodynamic histories are accompanied by pronounced differences in the timescales over which the pathways acquire moisture. Pfahl et al. (2014) showed that approximately 80% of WCB inflow moisture is acquired within about five days prior to WCB inflow. Figure 2b demonstrates that this characteristic timescale depends strongly on the inflow pathway. Air parcels of subtropical origin acquire moisture gradually over the 10 days preceding WCB inflow, reaching approximately 80% of their total moisture uptake around six days before inflow. In contrast, CAO air parcels acquire moisture much more rapidly, reaching the same fraction only about two days before inflow. Fast descent trajectories exhibit similarly rapid moisture uptake, although slightly slower than CAO trajectories, whereas slow descent trajectories more closely resemble the subtropical pathway.

These differences are consistent with the dominant moistening mechanisms and with the contrasting thermodynamic histories shown in Fig. 2a. CAO and fast descent trajectories transport relatively dry air toward the ocean surface, where large humidity and temperature contrasts drive intense surface latent heat fluxes, leading to rapid moistening. In contrast, subtropical trajectories remain within the moist subtropical boundary layer, where moisture is accumulated more gradually over several days. The slow descent pathway exhibits an intermediate behavior, reflecting its weaker dynamical descent and more prolonged residence in the lower troposphere.

Thus, despite all reaching the lower troposphere by the time of maximum uptake, the four pathways arrive there through fundamentally different thermodynamic transformations and acquire their moisture over substantially different timescales. The proposed classification captures these distinct physical pathways while remaining exhaustive and mutually exclusive. It therefore provides a physically interpretable framework for attributing WCB moisture to different source processes and for distinguishing the mechanisms and timescales through which moisture is supplied to WCB inflow.

3.4 Spatial distribution of pathways

Figure 3 shows the spatial distribution of WCB trajectories at inflow for each pathway. To first order, the inflow location does not determine the moistening pathway in the North Atlantic, as the four distributions largely overlap. The CAO pathway contributes somewhat more frequently to inflows northeast of the climatological maximum. In contrast, the subtropical origin pathway extends less far north and dominates WCB inflows over the Gulf of Mexico.

Although the inflow locations of the different pathways overlap substantially, their moisture source regions are more clearly separated. The CAO pathway acquires most of its moisture along the Gulf Stream SST front, where cold continental air is advected over the warm ocean. Moisture uptake associated with the fast descent pathway is more broadly distributed across

https://doi.org/10.5194/egusphere-2026-5486
Preprint. Discussion started: 22 September 2026

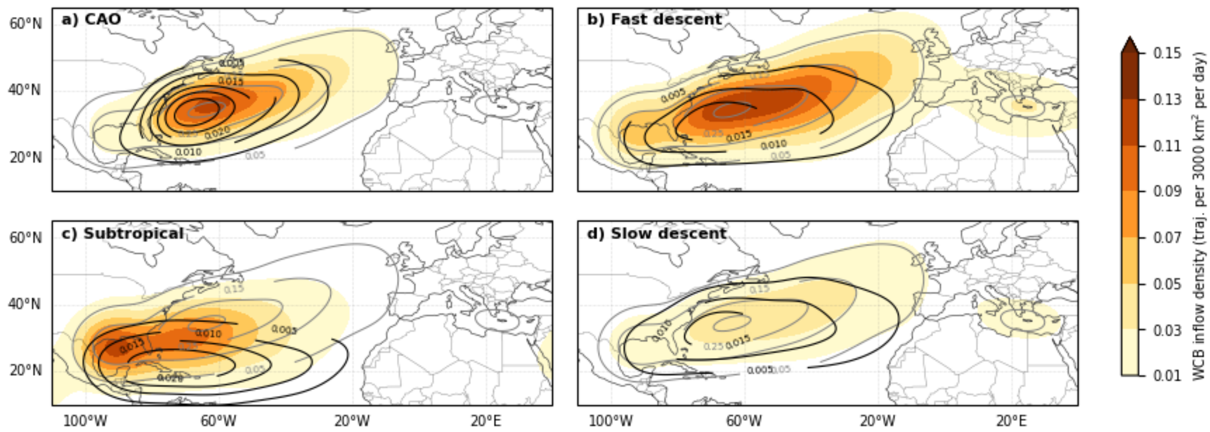

Figure 3. Climatological distribution of WCB inflow trajectory locations for (a) CAO, (b) fast descent, (c) subtropical origin, and (d) slow descent (color shading). Gray contours show the distribution of all WCB inflow trajectories combined (0.05, 0.15, 0.25, 0.35 traj. per 3000 km^2 per day), while black contours indicate the moisture uptake density for each pathway (0.005 to 0.030 % per 3000 km^2 with 0.005 intervals).

the North Atlantic, with substantial contributions from the central North Atlantic. In contrast, air parcels of subtropical origin acquire most of their moisture over the subtropical Atlantic, with a pronounced maximum over the Caribbean.

The strong spatial overlap of the WCB inflow pathways is a distinctive feature of the North Atlantic. In the larger North Pacific storm track, the pathways exhibit a clearer geographical separation (Fig. S1 in the Supplement). The CAO pathway is primarily associated with the Kuroshio SST front, whereas fast-descending air parcels preferentially feed WCB inflows farther downstream over the eastern North Pacific. The subtropical origin pathway contributes mainly to WCB inflows over the central North Pacific. Notably, subtropical origin air contributes little to WCB inflows near the entrance of the North Pacific storm track, in contrast to the North Atlantic.

This comparison highlights the North Atlantic as a particularly useful region for investigating the processes controlling WCB inflow characteristics. In the North Pacific, pathway occurrence is strongly constrained by geographical location, whereas in the North Atlantic the pathways overlap extensively and can contribute jointly to WCBs forming in the same region. Similar WCB inflow locations can therefore arise from markedly different transport and moistening histories.

4 What sets WCB inflow moisture content

The substantial overlap of the inflow pathways in the North Atlantic raises the question of why some WCBs are considerably moister than others. In particular, high inflow moisture may arise because moist WCBs contain a larger fraction of intrinsically moist pathways, such as air of subtropical origin, or because air arriving through each pathway is itself moister. We separate these two contributions by comparing WCBs in the moist and dry tails of the inflow moisture distribution.

https://doi.org/10.5194/egusphere-2026-5486
Preprint. Discussion started: 22 September 2026

4.1 Decomposing mean and composition effects

To investigate what controls WCB inflow moisture, we shift from individual trajectories to WCB objects, defined as coherent clusters of inflow trajectories associated with the same weather system. The absolute mean specific humidity of a WCB is strongly constrained by its geographical location, primarily through the large-scale meridional humidity gradient. A comparison based on absolute specific humidity would therefore largely separate WCBs occurring in climatologically warm and humid regions from those occurring farther poleward, rather than isolate the processes responsible for moisture variability among WCBs in a given region. We instead ask why some WCBs are anomalously moist or dry relative to other WCBs occurring at similar locations.

To remove this geographical dependence, we construct a local climatology of WCB-mean specific humidity on a coarse $2^\circ \times 2^\circ$ longitude–latitude grid. Each WCB object is assigned to the nearest grid point, and its specific humidity anomaly is calculated relative to the corresponding local climatological mean. We then define local moisture quantiles using a sliding $5^\circ \times 3^\circ$ longitude–latitude window. Within each window, WCB objects are classified into a moist tail (upper 10%), a median group (40th–60th percentile), and a dry tail (lower 10%) according to their specific humidity anomalies. To ensure robust estimates of the tails, the classification is performed only for windows containing at least 500 WCB objects.

We then quantify what accounts for the difference in mean specific humidity between each tail and the median group. The mean specific humidity of a WCB object, $\overline{q}$, can be expressed as the sum of the contributions from the four inflow pathways,

$$\overline{q} = \sum_c f_c \mu_c, \tag{1}$$

where f_c is the fractional contribution of pathway c to the WCB object and μ_c is its mean specific humidity. Differences in $\overline{q}$ can therefore arise in two ways: through changes in pathway composition, f_c, or through changes in the mean specific humidity within the individual pathways, μ_c. We separate these contributions by writing the difference between a tail group (t) and the median group (m) as

$$\Delta\overline{q} = \sum_c \left(f_c^t \mu_c^t - f_c^m \mu_c^m\right) = \underbrace{\sum_c \left(f_c^t - f_c^m\right)\mu_c^t}_{\text{pathway composition}} + \underbrace{\sum_c f_c^m \left(\mu_c^t - \mu_c^m\right)}_{\text{pathway mean}} \tag{2}$$

The first term measures the contribution from changes in the relative abundance of the four pathways, while the second measures the contribution from differences in their mean specific humidity.

Figure 4 summarizes the decomposition for North Atlantic WCBs. Moist and dry WCBs differ substantially in their pathway composition (Fig. 4a), particularly in the relative contributions of the CAO and subtropical origin pathways. Moist WCBs are predominately fed by air parcels of subtropical origin and fast descent. In contrast, dry WCBs are largely fed through the CAO pathway and almost no subtropical origin.

The question is whether this pronounced shift in pathway composition explains the corresponding anomalies in WCB inflow specific humidity. For this to be the case, replacing CAO air parcels with air parcels of subtropical origin would need to substantially increase the mean inflow specific humidity. Figure 4b shows the mean specific humidity within each pathway

https://doi.org/10.5194/egusphere-2026-5486
Preprint. Discussion started: 22 September 2026

for the different quantile groups. Air parcels of subtropical origin are generally moister than those associated with the CAO pathway, consistent with some expected contribution from the compositional shift. However, a stronger signal emerges within the pathways themselves: for all four pathways, air parcels associated with moist WCBs are systematically moister than those associated with median WCBs. Conversely, all four pathways are drier in the dry WCB group.

The formal decomposition in Eq. 2 quantifies these two effects. For moist relative to median WCBs (Fig. 4c), the composition term is negative for the CAO pathway and positive for the subtropical origin pathway, consistent with the shift in pathway fractions shown in Fig. 4a. These opposing contributions, however, largely cancel. Despite their different source regions and transport histories, the difference in mean inflow specific humidity between CAO and subtropical origin air parcels is too small for their redistribution to produce a large net moisture anomaly. The compositional shift therefore primarily replaces CAO-sourced air parcels with subtropical origin air parcels, with only a small net effect on WCB-mean specific humidity.

In contrast, the within-pathway moisture contribution is positive for all four pathways and together accounts for most of the positive specific humidity anomaly of moist WCBs. Thus, moist WCBs are not primarily moist because they contain more air parcels from climatologically moister pathways. Rather, air parcels arriving through each of the four pathways are themselves anomalously moist. The dry tail exhibits the complementary behavior (Fig. 4d): subtropical origin air parcels are replaced by CAO air parcels, but the net compositional effect remains small, while air parcels from all four pathways are anomalously dry. These effects are spatially robust throughout the North Atlantic storm track (Fig. S2 in the Supplement).

4.2 Moist WCBs take up their moisture earlier

Why do air parcels from all four pathways arrive systematically moister in moist WCBs? To address this question, we examine the evolution of moisture uptake and latitude along the WCB inflow trajectories prior to inflow (Fig. 5). For the CAO and fast descent pathways (Fig. 5a,b), moisture uptake increases rapidly toward WCB inflow and reaches a distinct maximum before $t = 0$, except for fast descent trajectories associated with dry WCBs. This concentration of moisture uptake close to inflow is consistent with the relatively short uptake timescales identified in Fig. 2b. However, the timing of the maximum differs systematically among the moisture quantile groups. For moist WCBs, moisture uptake peaks approximately two days before inflow, whereas the peak shifts progressively closer to $t = 0$ with decreasing inflow specific humidity. This shift in moisture uptake is accompanied by a systematic difference in the meridional transport of the trajectories. Air parcels feeding moist WCBs move equatorward earlier and reach lower latitudes than their drier counterparts. They exhibit a pronounced recirculation, first moving equatorward of their eventual inflow latitude before returning poleward toward the WCB inflow region. In contrast, trajectories feeding dry WCBs approach the inflow latitude more directly, with substantially less equatorward displacement. CAO trajectories also originate systematically farther north than fast descent trajectories, consistent with their lower initial potential temperature (Fig. 2a).

A somewhat different behavior is found for the slow descent and subtropical origin pathways (Fig. 5c,d). Here, the maximum moisture uptake occurs relatively close to inflow across all moisture quantile groups, and its timing varies less systematically with inflow specific humidity. Instead, the main distinction lies in the duration of moisture uptake. Trajectories associated with moist WCBs experience substantial moisture uptake over a longer period prior to inflow, whereas uptake for dry WCBs is more

https://doi.org/10.5194/egusphere-2026-5486
Preprint. Discussion started: 22 September 2026

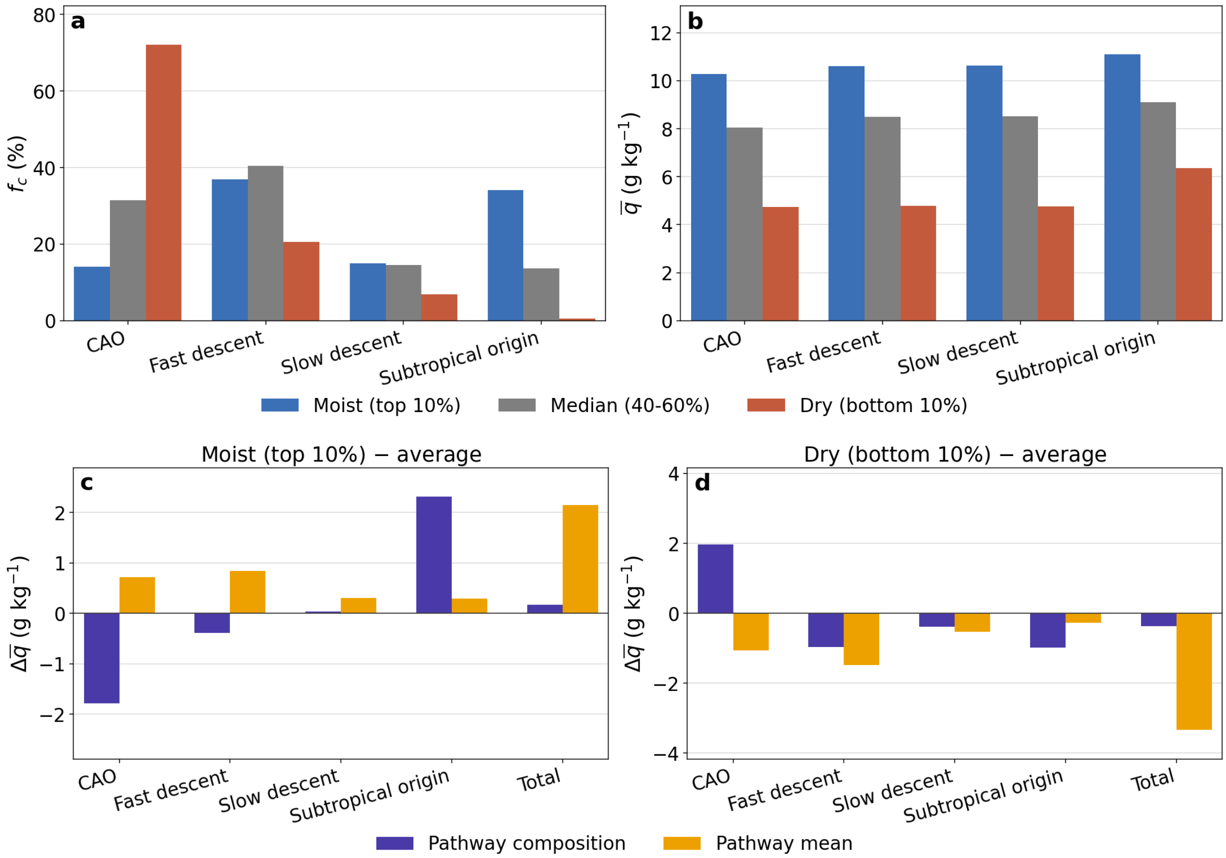

Figure 4. Pathway composition versus pathway mean specific humidity effects on WCB-mean specific humidity in moist and dry WCBs compared to median WCBs. WCB objects are ranked by their inflow specific humidity anomaly relative to the local WCB inflow climatology, and split into moist (top 10%), median (40–60%) and dry (bottom 10%) samples. All quantities are domain averages over 85°W–10°W, 25°N–60°N, weighted by the number of events per box. (a) Average fractional contribution of each pathway to WCB inflows in each quantile group (f_c). (b) Pathway-mean inflow specific humidity (μ_c). (c, d) Decomposition of the moist-minus-median (c) and dry-minus-median (d) difference in mean inflow humidity ($\overline{q}$) into the pathway composition term and the pathway mean term in Eq. 2. "Total" is the sum over the four pathways.

325 strongly concentrated near $t = 0$. This prolonged moistening is again accompanied by systematic differences in the meridional trajectory path. Both slow descent and subtropical origin air parcels feeding moist WCBs spend more time at lower latitudes and approach the inflow region from farther south than their drier counterparts. For the subtropical origin pathway, trajectories feeding dry WCBs are exported poleward from the subtropics considerably earlier, whereas those feeding moist WCBs remain at subtropical latitudes until closer to inflow. The higher inflow specific humidity of moist WCBs is therefore associated with
330 both more prolonged moisture uptake and longer residence at lower latitudes.

https://doi.org/10.5194/egusphere-2026-5486
Preprint. Discussion started: 22 September 2026

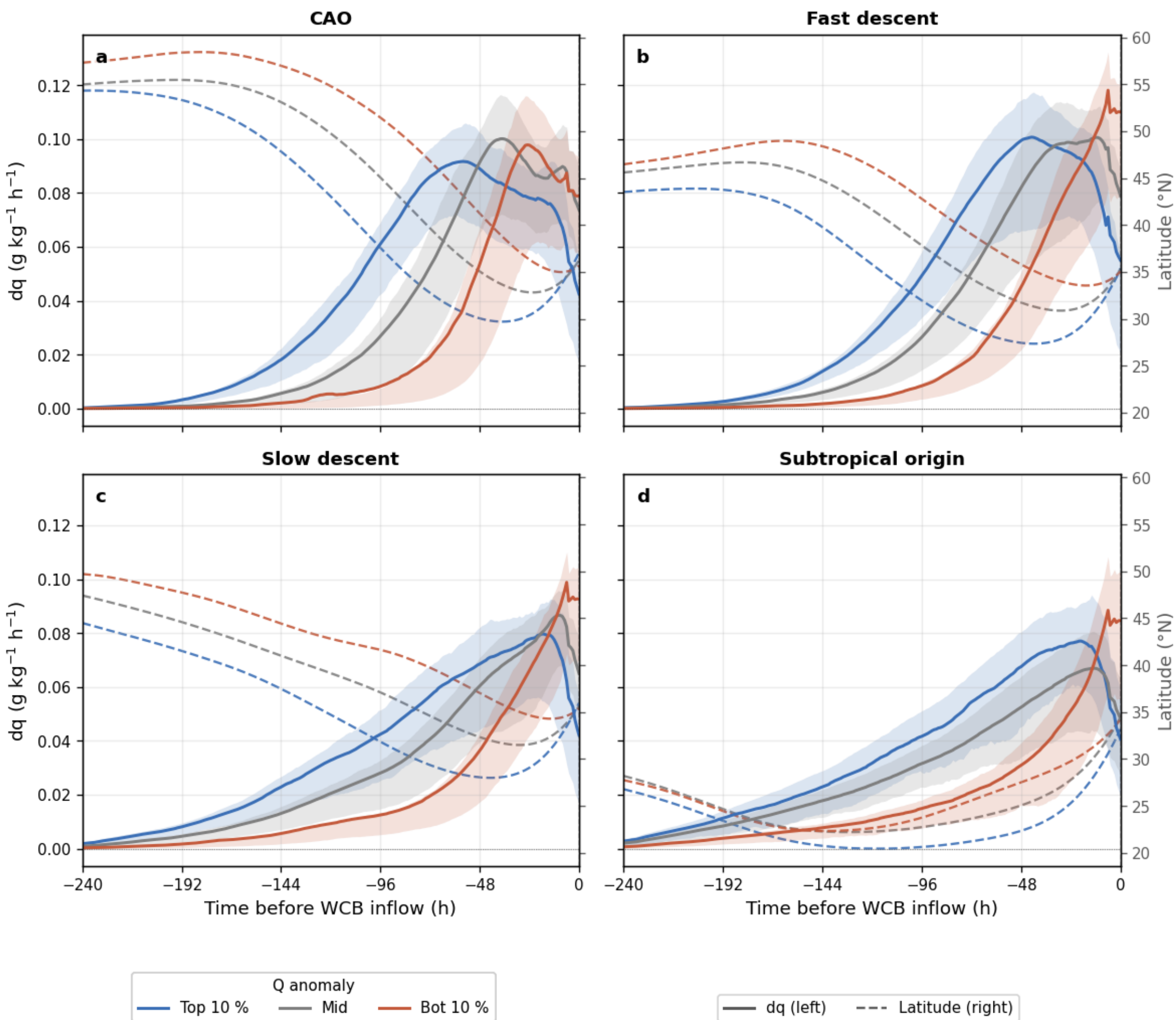

Figure 5. $q_{t=0}$-weighted North Atlantic mean backward time series of moisture uptake $\mathrm{d}q$ (solid lines, left axis; 12-h running mean; shading denotes the 25th–75th percentile range across grid boxes) and parcel latitude (dashed lines, right axis) for the (a) CAO, (b) fast descent, (c) slow descent, and (d) subtropical origin pathways. Colors denote the inflow specific humidity anomaly classes: upper 10% (red), 40th–60th percentiles (orange), and lower 10% (purple). The time $t = 0$ marks WCB inflow.

Despite these pathway specific differences, a coherent picture emerges across all four pathways. Air parcels feeding moist WCBs acquire a larger fraction of their moisture earlier in their history, whereas moisture uptake in dry WCBs is shifted toward the final hours before inflow. Indeed, close to $t = 0$, moisture uptake in dry WCBs can exceed that in moist WCBs, indicating that strong late uptake does not compensate for the absence of earlier moistening. Moist WCB inflows are therefore distinguished by moisture preconditioning well before the onset of WCB ascent, whereas dry inflows rely more strongly on

https://doi.org/10.5194/egusphere-2026-5486
Preprint. Discussion started: 22 September 2026

moisture acquired shortly before ascent. This temporal separation provides a common explanation for the within-pathway moisture anomalies identified in Fig. 4. Importantly, the earlier moistening of moist WCBs is closely linked to their meridional transport history. Across the pathways, moist WCB trajectories either recirculate farther equatorward or remain at low latitudes for longer before returning poleward into the extratropical WCB inflow region. This exposes the air parcels for longer to the warmer lower latitude environment and provides favorable conditions for earlier and more sustained moisture uptake.

The form of this preconditioning nevertheless differs among the pathways. For the CAO and fast descent pathways, it is expressed primarily through an earlier maximum in moisture uptake associated with a stronger equatorward excursion and subsequent poleward return. For the slow descent and subtropical origin pathways, the distinction is instead characterized by longer residence at low latitudes and more sustained moisture uptake prior to WCB inflow.

4.3 Moist and dry inflows along a shared thermodynamic route

The earlier and more prolonged moisture uptake of moist WCBs (Fig. 5) leaves their inflow air in a systematically different thermodynamic state before ascent. To characterize this state, we examine the trajectory evolution in relative humidity–temperature (RH–T) space (Fig. 6). Specific humidity depends on both temperature, through the saturation specific humidity q_s set by the Clausius–Clapeyron relation, and relative humidity, which measures the degree of saturation. RH–T space therefore allows differences in q to be interpreted in terms of temperature differences at a given RH or RH differences at a given temperature, while the isolines of constant q in Fig. 6 show how these two effects combine to determine the actual moisture content.

The four pathways trace distinct routes through RH–T space. Air in the CAO pathway (Fig. 6a) first evolves toward higher temperature while RH increases only gradually, consistent with the strong surface heat and moisture fluxes acting on cold and dry air advected over warmer water. Despite the rapid rise in q_s that accompanies this warming, RH does not fall correspondingly, indicating that moisture is supplied fast enough for q to increase together with temperature. About one day before inflow the moistening phase ends, and the trajectories turn toward higher RH along isolines of approximately constant q as the air returns poleward toward the inflow region (Fig. 5a); the subsequent RH increase therefore reflects cooling rather than continued uptake. The subtropical origin pathway (Fig. 6d) follows a contrasting route, along which temperature changes little while RH rises substantially, so that its increase in specific humidity stems from approaching saturation rather than from warming. The fast descent and slow descent pathways (Fig. 6b,c) occupy an intermediate regime in which warming and increasing RH contribute comparably. These routes extend the transformation perspective of Fig. 2: whereas θ–T space distinguishes the diabatic and vertical transformations of the air masses, RH–T space shows how those transformations set the moisture content reached before inflow.

Within each pathway, air feeding moist and dry WCBs follows essentially the same route through RH–T space. The two groups therefore do not undergo fundamentally different thermodynamic transformations, but differ in how far along this shared route they progress before ascent begins. Air feeding moist WCBs advances farther along the warming and moistening branch, largely completing the transformation characteristic of its pathway and reaching inflow warmer and closer to saturation. Air feeding dry WCBs is instead incorporated into the ascent at an earlier stage of the same route, so that its transformation is cut

https://doi.org/10.5194/egusphere-2026-5486
Preprint. Discussion started: 22 September 2026

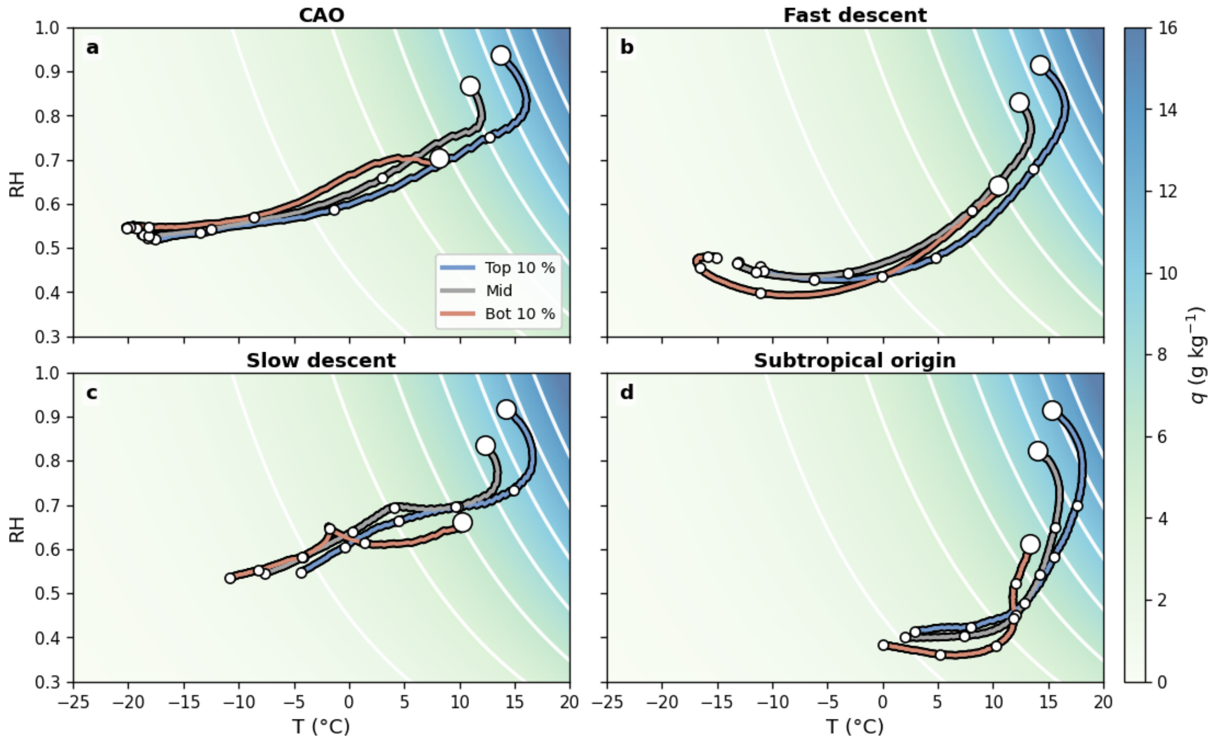

Figure 6. Thermodynamic $\mathrm{RH}-T$ diagram showing the median evolution of the (a) CAO, (b) fast descent, (c) slow descent and (d) subtropical origin pathways, separated into the tail and median quantile groups. Shading and white contours show specific humidity in the $\mathrm{RH}-T$ space derived from the Clausius-Clapeyron relation. The large white dots indicate the WCB inflow time, with small white dots marking 48 hour intervals.

short by the onset of ascent and its inflow air remains colder and farther from saturation. The moisture anomaly at inflow thus reflects how far each group has advanced along a common route rather than a difference between routes.

This difference is most cleanly read at the end of the active moistening phase, before the trajectories turn along the constant-q isolines, because the further RH increase toward inflow reflects cooling common to both groups. The relative contributions of temperature and relative humidity to the separation between the moist and dry groups vary by pathway: for the CAO and fast descent pathways it is carried mainly by temperature, whereas for the subtropical origin pathway it appears predominantly in RH, with moist inflow air reaching substantially closer to saturation.

This state space view complements the temporal evolution in Fig. 5. The earlier and more prolonged uptake of moist WCB air allows it to advance farther along its pathway route before ascent, whereas the shorter and later uptake of dry WCB air leaves the transformation cut short at inflow. The four pathways therefore define distinct thermodynamic routes, and within each route the degree of preconditioning sets how far the air progresses before it is incorporated into WCB ascent.

https://doi.org/10.5194/egusphere-2026-5486
Preprint. Discussion started: 22 September 2026

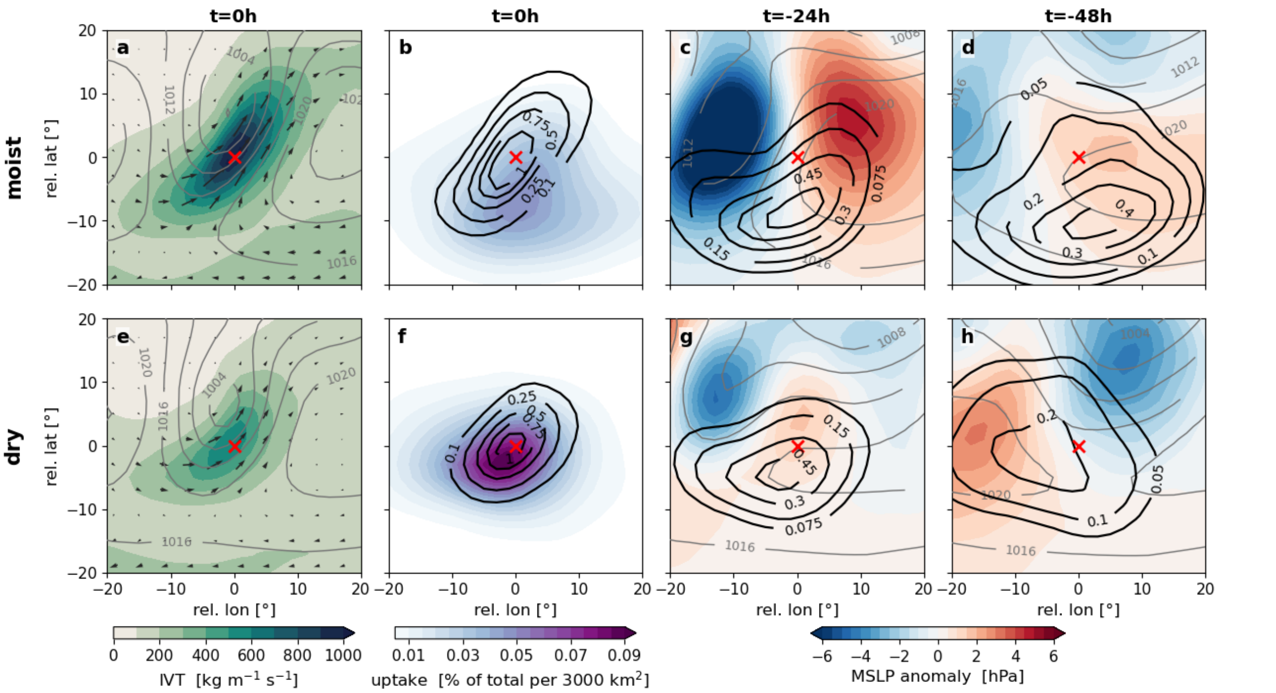

Figure 7. Synoptic setting and moisture sources of moist (top) and dry (bottom) WCB inflows over the North Atlantic for the 500 largest WCB inflow objects by trajectory count in each quantile group. All panels are shown in WCB inflow-relative coordinates, with $(0°, 0°)$ corresponding to the longitude and latitude of each WCB inflow. (a,d) Integrated vapor transport (IVT; shading and vectors) and MSLP (grey contours) at the time of WCB inflow. (b,e) Integrated moisture uptake along the 10-day backward trajectories (shading), expressed as a fraction of total inflow moisture per 3000 km^2, with trajectory density shown by contours (trajectories per 3000 km^2). The last two columns show MSLP anomalies (shading), absolute MSLP (grey contours), and trajectory density (black contours) (c,g) 24 h and (d,h) 48 h before WCB inflow. The red cross marks the composite-relative WCB inflow position.

4.4 Moist and dry WCB inflows emerge from distinct antecedent circulation

We next place this Lagrangian preconditioning in its synoptic context. Figure 7 shows inflow-centered composites of the 500 largest dry and moist WCB inflows by trajectory count. At the time of inflow, moist and dry WCBs are embedded in broadly similar mean sea level pressure (MSLP) patterns (Fig. 7a,e). In both groups, the inflow lies within a corridor of enhanced integrated vapor transport (IVT), between lower pressure to the northwest and higher pressure to the southeast. Such corridors constitute the strong poleward moisture transport from which WCB ascent draws its inflow air (Dacre et al., 2019). The moisture transport itself, however, differs substantially between the two groups. Moist WCBs are associated with considerably stronger IVT. The IVT is also more strongly oriented poleward for moist inflows, whereas transport into dry WCBs is weaker and more zonal. Thus, the pronounced moisture contrast at inflow is accompanied by a large difference in vapor transport despite comparatively small differences in the contemporaneous pressure pattern.

https://doi.org/10.5194/egusphere-2026-5486
Preprint. Discussion started: 22 September 2026

The moisture source distributions provide a Lagrangian perspective on how the air entering these transport corridors acquired its moisture (Fig. 7b,f). For both groups, most moisture uptake occurs relatively close to the eventual WCB inflow region rather than in geographically remote source regions. This is consistent with previous Lagrangian analyses showing that strong midlatitude vapor transport can contain substantial moisture acquired recently within the extratropics rather than transported directly from the subtropics (Sodemann and Stohl, 2013; Pfahl et al., 2014; Ramos et al., 2016). The source distributions are nevertheless systematically displaced. For dry WCBs, uptake remains highly concentrated close to the inflow and extends upstream of it, whereas for moist WCBs it is shifted equatorward, its peak lies farther from the eventual inflow and the uptake is spread over a larger area. This greater separation between the dominant uptake region and the inflow indicates that moist WCB parcels are moistened well before reaching the inflow and are transported poleward already moist, whereas dry WCB parcels acquire much of their moisture near the inflow shortly before ascent. The spatial pattern is therefore consistent with the difference in uptake timing identified in Fig. 5.

The antecedent circulation differs markedly between moist and dry WCBs. At 48h before inflow (Fig. 7d,h), trajectories feeding dry WCBs are located southwest of a low pressure system, within a strong southwesterly–northeasterly pressure gradient that drives cold air advection over the North Atlantic. This circulation is characteristic of a CAO and places the trajectories within the cold sector of the preceding cyclone as they approach the future WCB inflow region. No comparable CAO signature is apparent for moist WCBs at this lag. Instead, during their period of enhanced antecedent moisture uptake, the trajectories lie on the equatorward flank of a broad high pressure system. Their position is consistent with the stronger equatorward excursion and subsequent poleward recirculation identified in Fig. 5. The prolonged preconditioning of moist WCB air (Fig. 5) therefore occurs within a distinctly different antecedent circulation from the late uptake associated with dry WCBs. Finally, trajectories feeding the moist WCB inflows approach the inflow region by recirculating anticylonically around a high pressure system (Fig. 7c), reflecting the pattern illustrated in the case study (Fig. 1). In contrast, trajectories approach the dry inflows directly from the northwest without a pronounced anticyclonic recirculation (Fig. 7g).

The similarity of the pressure fields at inflow consequently masks substantially different upstream histories. Dry WCB air approaches the inflow region within a relatively recent CAO and acquires much of its moisture shortly before ascent. Moist WCB air, by contrast, has already undergone substantial conditioning while circulating along the equatorward flank of the antecedent high pressure system. By the onset of WCB ascent, these different histories converge into broadly similar pressure configurations, while their accumulated thermodynamic differences remain evident in the substantially stronger and more poleward vapor transport associated with moist WCBs. Together with Figs. 5 and 6, these composites demonstrate that the moisture content of the air entering strong vapor transport corridors depends on its antecedent thermodynamic history, which is not apparent from the instantaneous pressure configuration at WCB inflow.

https://doi.org/10.5194/egusphere-2026-5486
Preprint. Discussion started: 22 September 2026

5 Discussion

5.1 Preconditioning of storm track moisture supply

Our results place the moisture handover between successive weather systems into a climatological framework. Previous studies have shown that air moistened in the cold sector of one cyclone can subsequently feed the warm sector and WCB of an upstream cyclone (Sodemann and Stohl, 2013; Dacre et al., 2019; Papritz et al., 2021; Demirdjian et al., 2023). The case study (Fig. 1) illustrates how this handover is accomplished: initially distinct extratropical and subtropical air masses converge on the equatorward flank of an anticyclone, recirculate within a coherent feeder airstream, and are subsequently incorporated into WCB inflow. The pathway analysis shows that this feeder airstream is not associated with a single moisture source or air-mass origin. Instead, it assembles air that has undergone different transformations, ranging from rapid moistening of cold or descending extratropical air to more gradual conditioning of air residing in the lower-latitude boundary layer.

The pathway-dependent uptake timescales quantify the memory inherent in this moisture handover (Fig. 2). CAO and fast descent air parcels acquire much of their moisture within approximately two days of WCB inflow, whereas slow descent and subtropical origin air integrate moisture uptake over substantially longer periods. The moisture delivered to a WCB can therefore reflect storm track evolution over several preceding days rather than only conditions in the immediate vicinity of the ascending cyclone, consistent with the results of the idealized experiments of Demirdjian et al. (2023). Moreover, the moist–dry comparison shows that the duration and timing of this upstream conditioning exert a stronger control on the eventual inflow humidity than the mixture of pathways itself (Fig. 5). This contrast is illustrated schematically in Fig. 8. For moist WCBs, stronger and more explicit equatorward recirculation allows moisture to be acquired earlier and the pathway-specific thermodynamic transformation to proceed further before ascent. This recirculation organizes a coherent feeder airstream (Fig. 8a), which is subsequently recirculated on the equatorward flank of a high pressure system (Fig. 8b) and fed into the warm sector of the upstream cyclone (Fig. 8c). In contrast, dry WCB inflow is more commonly supplied by recent CAO-related uptake (Fig. 8d) without pronounced recirculation around an anticyclone (Fig. 8e). The corresponding feeder airstream is therefore more directly tied to the cyclone-relative circulation, in the sense that the cyclone catches up with the preconditioned air (Fig. 8f), consistent with the configuration described by Dacre et al. (2019). Feeder airstreams can thus emerge from distinct dynamical configurations, with consequences for the timescale and thermodynamic history over which the moisture supply to subsequent WCBs is assembled.

The contrasting configurations summarized in Fig. 8 highlight the role of anticyclonic circulation in establishing moist WCB inflow. Anticyclones can provide an environment in which air remains at lower latitudes, acquires moisture over several days, and is subsequently recirculated into the feeder airstream of an upstream cyclone. This pathway differs from the more direct moisture handover associated with recent CAO conditions in dry WCBs and suggests that the persistence and structure of the antecedent anticyclonic circulation may regulate the degree of moisture preconditioning. This interpretation is consistent with Okajima et al. (2024), who found enhanced oceanic moisture supply within anticyclonic domains and a climatological net transport of moisture from anticyclonic into cyclonic domains.

https://doi.org/10.5194/egusphere-2026-5486
Preprint. Discussion started: 22 September 2026

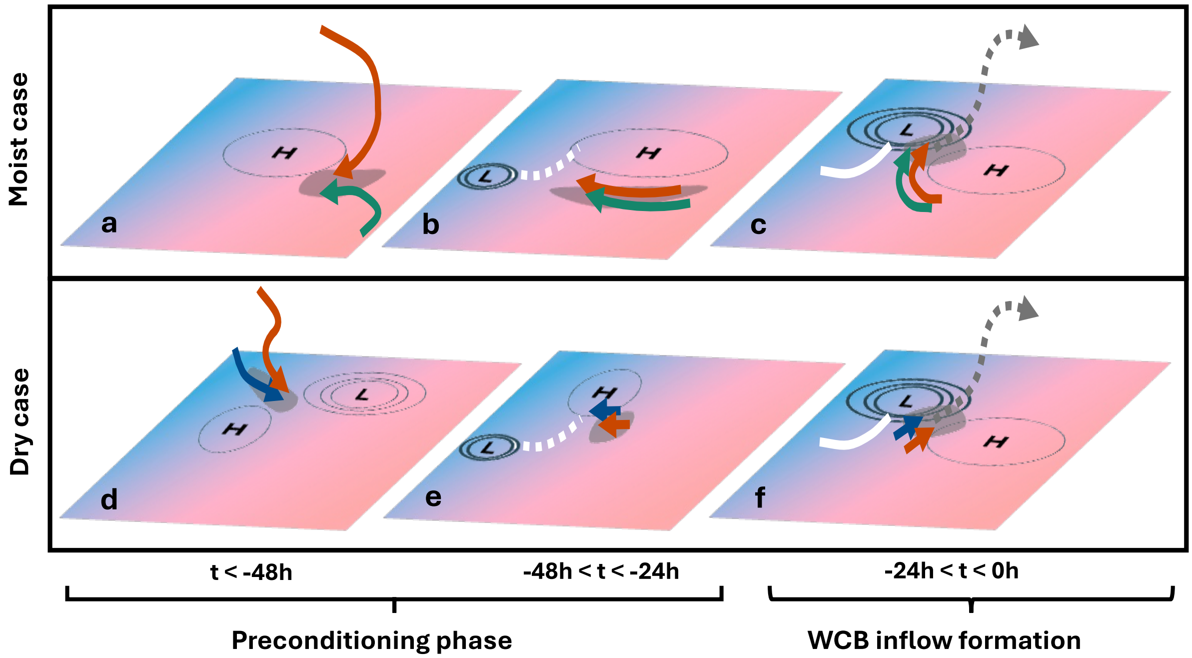

Figure 8. Schematic of moisture preconditioning for moist and dry WCB inflows. Moist case (first row): prolonged preconditioning along the subtropical flank of an anticyclone (a,b) supplies the subsequent WCB ascent (c). Dry case (second row): moisture uptake during a preceding CAO (d,e) supplies the subsequent WCB ascent (f). Future WCB ascent is indicated by a grey dashed arrow. Shading indicates SST, increasing from blue to red, while grey shading marks the location of WCB inflow air parcels. Arrows show the mean spatiotemporal evolution of these parcels for the CAO (blue), fast descent (orange), and subtropical origin (green) pathways. The bold low pressure system denotes the cyclone associated with eventual WCB ascent, and the white line shows its future (dashed) and past (solid) track with respect to the panel time.

This relationship suggests a possible connection between WCB moisture supply and the upper-level dynamics governing anticyclone persistence. Rossby wave breaking and blocking organize persistent anticyclonic flow (Tamarin-Brodsky and Harnik, 2024; Tamarin-Brodsky et al., 2026) and can themselves be promoted by latent heating within WCBs (Pfahl et al., 2015; Steinfeld and Pfahl, 2019; Yamamoto et al., 2021; Wenta et al., 2024). If such circulation states also prolong the equatorward residence and preconditioning of air subsequently entering WCBs, they could provide a dynamical memory linking latent heating in successive weather systems. This would constitute a potential feedback within the storm track: WCB latent heating contributes to ridge amplification and anticyclonic persistence, while the resulting circulation may in turn precondition the moisture supply available for latent heating in subsequent WCBs. An important question is therefore which configurations of successive baroclinic waves, and which large-scale circulation regimes, are most conducive to this preconditioning. This dependence on the preceding flow evolution also has implications for predictability, as errors in WCB moisture may originate several days before ascent. This dynamical control on preconditioning may likewise be relevant in a warmer climate: global

https://doi.org/10.5194/egusphere-2026-5486
Preprint. Discussion started: 22 September 2026

warming increases the moisture potentially available to WCBs (Joos et al., 2023), while changes in storm track dynamics may alter the pathways and residence times through which that moisture is acquired. Establishing these connections explicitly would require relating the pathway and preconditioning statistics diagnosed here to Rossby wave breaking, blocking, and their changes across circulation regimes and climates.

5.2 Preconditioning of atmospheric river moisture

The connection between WCB inflow and corridors of strong vapor transport extends these results to atmospheric rivers (ARs), although WCB inflow and ARs describe distinct features of the cyclone circulation (Dacre et al., 2019). Our results complement Lagrangian studies showing that substantial AR moisture can be acquired within the midlatitudes rather than transported directly from the subtropics (Sodemann and Stohl, 2013; Dacre et al., 2015; Ramos et al., 2016). They further show that the moisture content of air entering these transport corridors can retain a memory of its antecedent circulation. Strong vapor transport associated with WCB ascent may therefore reflect not only the instantaneous circulation, but also the preceding history of the air being transported.

This distinction is apparent in the moist–dry WCB comparison. At inflow, the pressure fields and associated low-level flow are broadly similar, whereas peak IVT is roughly 60% larger for moist WCBs (Fig. 7a,d). The similarity of the pressure fields suggests that this difference reflects the higher specific humidity, established through earlier and more prolonged moisture uptake, rather than a substantially stronger circulation. ARs have been characterized as moisture or wind dominated according to the relative contributions of specific humidity and wind speed to their instantaneous vapor transport (Gonzales et al., 2020). Our results suggest that the moisture-dominated character of such transport can itself be established earlier, through the thermodynamic transformation of the air before it is incorporated into the AR.

5.3 Limitations

Several limitations should be considered when interpreting our results. Lagrangian trajectories are less reliable within the boundary layer, where strong turbulent mixing and unresolved subgrid-scale motions limit the accuracy with which individual air parcels can be followed (Sodemann et al., 2008; Sodemann, 2020). The diagnosed locations and histories of moisture uptake should therefore be interpreted with greater caution when trajectories spend extended periods within the marine boundary layer.

We further neglect cloud processes. The brief diabatic cooling near 850 hPa common to all four pathways (Fig. 2a) is plausibly associated with cloud-radiative or evaporative processes, indicating that condensation and evaporation modify the parcels before ascent in ways that our diagnostic does not resolve. More generally, our attribution treats moisture loss as irreversible removal and therefore cannot represent moisture recycling, whereby condensate evaporates and is subsequently reincorporated into ascending air within the WCB itself.

Finally, inflow specific humidity is only one determinant of the diabatic impact of a WCB (Heitmann et al., 2024). The total latent heat release also depends on the mass of ascending air, the depth and rate of ascent, and the convective contribution to heating, all of which are influenced by the large-scale forcing for ascent rather than by moisture supply alone (Blanchard

https://doi.org/10.5194/egusphere-2026-5486
Preprint. Discussion started: 22 September 2026

et al., 2020; Oertel et al., 2025). Moist inflow favors strong latent heating but does not determine it uniquely. Our results should therefore be interpreted as constraining the moisture available for latent heating rather than the magnitude of the heating itself.

6 Conclusions

This study provides a Lagrangian framework for linking the upstream dynamical history of WCB inflow air to the moisture subsequently available for latent heating. Wintertime North Atlantic WCB inflow is a superposition of four distinct pathways—CAO, fast descent, slow descent, and subtropical origin—that differ in their thermodynamic evolution, moisture source regions, and uptake timescales. Most inflow moisture is of recent extratropical origin, while the characteristic time over which it is acquired ranges from about two days for the CAO and fast descent pathways to four to six days for the slow descent and subtropical origin pathways. The pathway therefore determines the route and memory timescale by which moisture reaches WCB inflow.

The mean moisture content of individual WCBs, however, is not primarily controlled by pathway composition. Although moist WCBs contain substantially more subtropical origin air and less CAO air than dry WCBs, these compositional changes contribute little to the inflow moisture *anomaly* because their effects largely cancel. Instead, air arriving through all four pathways is systematically moister in moist WCBs and drier in dry WCBs. Within each pathway, moist and dry inflows follow similar trajectories through RH–T space but reach different thermodynamic states before ascent, with moist inflow air progressing farther toward warmer and more saturated conditions. This difference is associated with earlier and more prolonged moisture uptake prior to WCB inflow.

The distinction between moist and dry WCBs is therefore established primarily during their antecedent evolution rather than through strongly different synoptic conditions at the onset of ascent. While their mean sea level pressure patterns are broadly similar at inflow, their preceding circulation and moisture histories differ substantially. Dry WCB air is commonly associated with a recent CAO and relatively late moisture uptake, while moist WCB air is preconditioned earlier during an equatorward excursion along the flank of an antecedent anticyclone. Thus, the moisture entering WCB ascent cannot be understood from the contemporaneous cyclone environment alone. Its origin must be traced over the days preceding ascent.

These findings raise a broader dynamical question: which configurations of the baroclinic wave are most effective at establishing the prolonged residence and recirculation that favor moist WCB inflow? Our results point particularly to the organization of successive weather systems and the phase relationship between the circulation that preconditions the inflow air and the cyclone in which it subsequently ascends. Characterizing when such configurations arise would help establish how the storm track regulates the moisture supply available for its own diabatic forcing. More fundamentally, our results show that the thermodynamic state entering a WCB is not determined solely by the cyclone in which ascent occurs, but retains a memory of the preceding evolution of the storm track.

Code and data availability. The ERA5 reanalysis data (Hersbach et al., 2020) used in this study are publicly available from the Copernicus Climate Change Service (C3S) Climate Data Store (https://doi.org/10.24381/cds.adbb2d4).

Appendix A: Illustration of the moisture source attribution

Figure A1 illustrates the moisture source attribution procedure of Sodemann et al. (2008) applied in this study. In this example, the parcel initially contains $2\,\mathrm{g\,kg^{-1}}$ and subsequently acquires $4\,\mathrm{g\,kg^{-1}}$ at $t = -192$h (Fig. A1a). A later 50 % moisture loss reduces both the initial moisture and this uptake contribution by 50 %. The final uptake of $3\,\mathrm{g\,kg^{-1}}$ at $t = -48$h experiences no subsequent loss and is therefore retained in full. Thus, although the first uptake event amounts to $4\,\mathrm{g\,kg^{-1}}$, only $2\,\mathrm{g\,kg^{-1}}$ of this uptake is attributed to the moisture present at WCB inflow, whereas the full $3\,\mathrm{g\,kg^{-1}}$ of the second uptake is attributed to the WCB inflow moisture (Fig. A1b).

Author contributions. MF conceived and designed the study, acquired the funding, conducted the analyses, prepared the figures, and wrote the original manuscript. TTB contributed to the conceptual development of the study, interpretation of the results, and review of the manuscript.

Competing interests. The authors declare that they have no conflict of interest.

Acknowledgements. We thank Michael Sprenger (ETH Zürich) for providing the WCB climatology and computing the backward trajectories on which this study is based. MF acknowledges funding from the Swiss National Science Foundation (SNSF) through grant P500PN_230407. Generative AI tools were used for language editing and coding assistance.

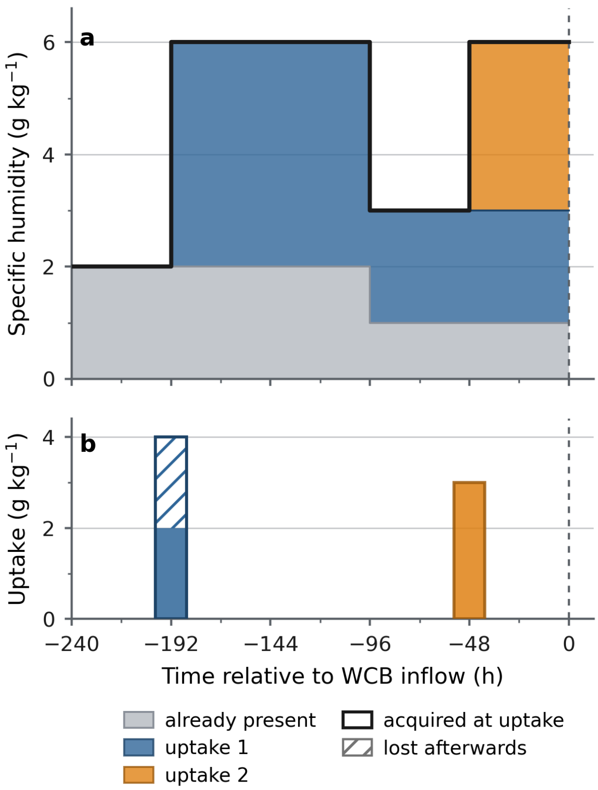

Figure A1. Illustration of the Lagrangian moisture source attribution procedure of Sodemann et al. (2008). (a) Example specific humidity evolution along a 10-day backward trajectory, showing moisture already present at the start of the trajectory and two subsequent uptake events. Colored areas indicate the portions of these contributions that remain after subsequent moisture losses and reach WCB inflow at $t = 0$. (b) Initially diagnosed uptake (full bar height) and the portion ultimately attributed to WCB inflow moisture (filled). Hatching indicates moisture subsequently lost from the parcel.

References

Aemisegger, F. and Papritz, L.: A Climatology of Strong Large-Scale Ocean Evaporation Events. Part I: Identification, Global Distribution, and Associated Climate Conditions, Journal of Climate, 31, 7287 – 7312, https://doi.org/10.1175/JCLI-D-17-0591.1, 2018.

Aemisegger, F., Vogel, R., Graf, P., Dahinden, F., Villiger, L., Jansen, F., Bony, S., Stevens, B., and Wernli, H.: How Rossby wave breaking modulates the water cycle in the North Atlantic trade wind region, Weather and Climate Dynamics, 2, 281–309, https://doi.org/10.5194/wcd-2-281-2021, 2021.

Ahmadi-Givi, F., Graig, G. C., and Plant, R. S.: The dynamics of a midlatitude cyclone with very strong latent-heat release, Quarterly Journal of the Royal Meteorological Society, 130, 295–323, https://doi.org/https://doi.org/10.1256/qj.02.226, 2004.

Binder, H., Boettcher, M., Joos, H., and Wernli, H.: The Role of Warm Conveyor Belts for the Intensification of Extratropical Cyclones in Northern Hemisphere Winter, Journal of the Atmospheric Sciences, 73, 3997 – 4020, https://doi.org/10.1175/JAS-D-15-0302.1, 2016.

Blanchard, N., Pantillon, F., Chaboureau, J.-P., and Delanoë, J.: Organization of convective ascents in a warm conveyor belt, Weather and Climate Dynamics, 1, 617–634, https://doi.org/10.5194/wcd-1-617-2020, 2020.

Catto, J. L. and Raveh-Rubin, S.: Climatology and dynamics of the link between dry intrusions and cold fronts during winter. Part I: global climatology, Climate Dynamics, 53, 1873–1892, https://doi.org/10.1007/s00382-019-04745-w, 2019.

Christ, S., Wenta, M., Grams, C. M., and Oertel, A.: From sea to sky: understanding the sea surface temperature impact on an atmospheric blocking event using sensitivity experiments with the ICOsahedral Nonhydrostatic (ICON) model, Weather and Climate Dynamics, 6, 17–42, https://doi.org/10.5194/wcd-6-17-2025, 2025.

Dacre, H. F., Clark, P. A., Martinez-Alvarado, O., Stringer, M. A., and Lavers, D. A.: How Do Atmospheric Rivers Form?, Bulletin of the American Meteorological Society, 96, 1243 – 1255, https://doi.org/10.1175/BAMS-D-14-00031.1, 2015.

Dacre, H. F., Martínez-Alvarado, O., and Mbengue, C. O.: Linking Atmospheric Rivers and Warm Conveyor Belt Airflows, Journal of Hydrometeorology, 20, 1183 – 1196, https://doi.org/10.1175/JHM-D-18-0175.1, 2019.

Demirdjian, R., Doyle, J. D., Finocchio, P. M., and Reynolds, C. A.: Preconditioning and Intensification of Upstream Extratropical Cyclones through Surface Fluxes, Journal of the Atmospheric Sciences, 80, 1499 – 1517, https://doi.org/10.1175/JAS-D-22-0251.1, 2023.

Federer, M., Papritz, L., Sprenger, M., Grams, C. M., and Wenta, M.: On the Local Available Potential Energy Perspective of Baroclinic Wave Development, Journal of the Atmospheric Sciences, 81, 871 – 886, https://doi.org/10.1175/JAS-D-23-0138.1, 2024.

Gonzales, K. R., Swain, D. L., Barnes, E. A., and Diffenbaugh, N. S.: Moisture- Versus Wind-Dominated Flavors of Atmospheric Rivers, Geophysical Research Letters, 47, e2020GL090 042, https://doi.org/https://doi.org/10.1029/2020GL090042, e2020GL090042 2020GL090042, 2020.

Grams, C. M., Wernli, H., Böttcher, M., Čampa, J., Corsmeier, U., Jones, S. C., Keller, J. H., Lenz, C.-J., and Wiegand, L.: The key role of diabatic processes in modifying the upper-tropospheric wave guide: a North Atlantic case-study, Quarterly Journal of the Royal Meteorological Society, 137, 2174–2193, https://doi.org/https://doi.org/10.1002/qj.891, 2011.

Grossman, R. L. and Betts, A. K.: Air–Sea Interaction during an Extreme Cold Air Outbreak from the Eastern Coast of the United States, Monthly Weather Review, 118, 324 – 342, https://doi.org/10.1175/1520-0493(1990)118<0324:AIDAEC>2.0.CO;2, 1990.

Guan, B. and Waliser, D. E.: Detection of atmospheric rivers: Evaluation and application of an algorithm for global studies, Journal of Geophysical Research: Atmospheres, 120, 12 514–12 535, https://doi.org/https://doi.org/10.1002/2015JD024257, 2015.

Heitmann, K., Sprenger, M., Binder, H., Wernli, H., and Joos, H.: Warm conveyor belt characteristics and impacts along the life cycle of extratropical cyclones: case studies and climatological analysis based on ERA5, Weather and Climate Dynamics, 5, 537–557, https://doi.org/10.5194/wcd-5-537-2024, 2024.

Hersbach, H., Bell, B., Berrisford, P., Hirahara, S., Horányi, A., Muñoz-Sabater, J., Nicolas, J., Peubey, C., Radu, R., Schepers, D., Simmons, A., Soci, C., Abdalla, S., Abellan, X., Balsamo, G., Bechtold, P., Biavati, G., Bidlot, J., Bonavita, M., De Chiara, G., Dahlgren, P., Dee, D., Diamantakis, M., Dragani, R., Flemming, J., Forbes, R., Fuentes, M., Geer, A., Haimberger, L., Healy, S., Hogan, R. J., Hólm, E., Janisková, M., Keeley, S., Laloyaux, P., Lopez, P., Lupu, C., Radnoti, G., de Rosnay, P., Rozum, I., Vamborg, F., Villaume, S., and Thépaut, J.-N.: The ERA5 global reanalysis, Quarterly Journal of the Royal Meteorological Society, 146, 1999–2049, https://doi.org/https://doi.org/10.1002/qj.3803, 2020.

Hoskins, B. J. and Valdes, P. J.: On the Existence of Storm-Tracks, Journal of Atmospheric Sciences, 47, 1854 – 1864, https://doi.org/10.1175/1520-0469(1990)047<1854:OTEOST>2.0.CO;2, 1990.

Hwang, Y., Yoo, C., Lee, S., Sprenger, M., and Federer, M.: Linking warm conveyor belts to the TEM circulation in Northern Hemisphere midlatitude winter, npj Climate and Atmospheric Science, 9, 164, https://doi.org/10.1038/s41612-026-01435-3, 2026.

https://doi.org/10.5194/egusphere-2026-5486
Preprint. Discussion started: 22 September 2026

Joos, H., Sprenger, M., Binder, H., Beyerle, U., and Wernli, H.: Warm conveyor belts in present-day and future climate simulations – Part 1: Climatology and impacts, Weather and Climate Dynamics, 4, 133–155, https://doi.org/10.5194/wcd-4-133-2023, 2023.

Knippertz, P. and Wernli, H.: A Lagrangian Climatology of Tropical Moisture Exports to the Northern Hemispheric Extratropics, Journal of Climate, 23, 987 – 1003, https://doi.org/10.1175/2009JCLI3333.1, 2010.

Knippertz, P., Wernli, H., and Gläser, G.: A Global Climatology of Tropical Moisture Exports, Journal of Climate, 26, 3031 – 3045, https://doi.org/10.1175/JCLI-D-12-00401.1, 2013.

Lojko, A., Prein, A. F., Ribeiro, B. Z., and Winters, A.: Warm-Conveyor Belt Persistence and Upstream Cyclone Tilt Shape the Predictability of a Rossby Wave Breaking Event, ESS Open Archive, 2025, https://doi.org/10.22541/essoar.175821720.04705853/v1, 2025.

Madonna, E., Wernli, H., Joos, H., and Martius, O.: Warm Conveyor Belts in the ERA-Interim Dataset (1979–2010). Part I: Climatology and Potential Vorticity Evolution, Journal of Climate, 27, 3 – 26, https://doi.org/10.1175/JCLI-D-12-00720.1, 2014.

Martínez-Alvarado, O., Joos, H., Chagnon, J., Boettcher, M., Gray, S. L., Plant, R. S., Methven, J., and Wernli, H.: The dichotomous structure of the warm conveyor belt, Quarterly Journal of the Royal Meteorological Society, 140, 1809–1824, https://doi.org/https://doi.org/10.1002/qj.2276, 2014.

Newell, R. E., Newell, N. E., Zhu, Y., and Scott, C.: Tropospheric rivers? – A pilot study, Geophysical Research Letters, 19, 2401–2404, https://doi.org/https://doi.org/10.1029/92GL02916, 1992.

Oertel, A., Boettcher, M., Joos, H., Sprenger, M., and Wernli, H.: Potential vorticity structure of embedded convection in a warm conveyor belt and its relevance for large-scale dynamics, Weather and Climate Dynamics, 1, 127–153, https://doi.org/10.5194/wcd-1-127-2020, 2020.

Oertel, A., Miltenberger, A. K., Grams, C. M., and Hoose, C.: Sensitivities of warm conveyor belt ascent, associated precipitation characteristics and large-scale flow pattern: Insights from a perturbed parameter ensemble, Quarterly Journal of the Royal Meteorological Society, 151, e4986, https://doi.org/https://doi.org/10.1002/qj.4986, 2025.

Okajima, S., Nakamura, H., and Spengler, T.: Midlatitude Oceanic Fronts Strengthen the Hydrological Cycle Between Cyclones and Anticyclones, Geophysical Research Letters, 51, e2023GL106 187, https://doi.org/https://doi.org/10.1029/2023GL106187, 2024.

Papritz, L. and Spengler, T.: A Lagrangian Climatology of Wintertime Cold Air Outbreaks in the Irminger and Nordic Seas and Their Role in Shaping Air–Sea Heat Fluxes, Journal of Climate, 30, 2717 – 2737, https://doi.org/10.1175/JCLI-D-16-0605.1, 2017.

Papritz, L., Pfahl, S., Sodemann, H., and Wernli, H.: A Climatology of Cold Air Outbreaks and Their Impact on Air–Sea Heat Fluxes in the High-Latitude South Pacific, Journal of Climate, 28, 342 – 364, https://doi.org/10.1175/JCLI-D-14-00482.1, 2015.

Papritz, L., Aemisegger, F., and Wernli, H.: Sources and Transport Pathways of Precipitating Waters in Cold-Season Deep North Atlantic Cyclones, Journal of the Atmospheric Sciences, 78, 3349 – 3368, https://doi.org/10.1175/JAS-D-21-0105.1, 2021.

Pauluis, O., Czaja, A., and Korty, R.: The Global Atmospheric Circulation on Moist Isentropes, Science, 321, 1075–1078, https://doi.org/10.1126/science.1159649, 2008.

Peixoto, J. P., Oort, A. H., Covey, C., and Taylor, K.: Physics of Climate, 1992.

Pfahl, S., Madonna, E., Boettcher, M., Joos, H., and Wernli, H.: Warm Conveyor Belts in the ERA-Interim Dataset (1979–2010). Part II: Moisture Origin and Relevance for Precipitation, Journal of Climate, 27, 27 – 40, https://doi.org/10.1175/JCLI-D-13-00223.1, 2014.

Pfahl, S., Schwierz, C., Croci-Maspoli, M., Grams, C. M., and Wernli, H.: Importance of latent heat release in ascending air streams for atmospheric blocking, Nature Geoscience, 8, 610–614, https://doi.org/10.1038/ngeo2487, 2015.

Pickl, M., Quinting, J. F., and Grams, C. M.: Warm conveyor belts as amplifiers of forecast uncertainty, Quarterly Journal of the Royal Meteorological Society, 149, 3064–3085, https://doi.org/https://doi.org/10.1002/qj.4546, 2023.

https://doi.org/10.5194/egusphere-2026-5486
Preprint. Discussion started: 22 September 2026

Quinting, J., Grams, C. M., Kirsch, B., Oertel, A., Ramos, A. M., Raveh-Rubin, S., and Schäfler, A.: Dry Intrusion Connects High-Impact Cyclones Eunice and Franklin: Emerging Observational Targets of NAWDIC, Bulletin of the American Meteorological Society, 107, E1302 – E1314, https://doi.org/10.1175/BAMS-D-25-0170.1, 2026.

Ralph, F. M., Neiman, P. J., Wick, G. A., Gutman, S. I., Dettinger, M. D., Cayan, D. R., and White, A. B.: Flooding on California's Russian River: Role of atmospheric rivers, Geophysical Research Letters, 33, https://doi.org/https://doi.org/10.1029/2006GL026689, 2006.

Ramos, A. M., Nieto, R., Tomé, R., Gimeno, L., Trigo, R. M., Liberato, M. L. R., and Lavers, D. A.: Atmospheric rivers moisture sources from a Lagrangian perspective, Earth System Dynamics, 7, 371–384, https://doi.org/10.5194/esd-7-371-2016, 2016.

Raveh-Rubin, S.: Dry Intrusions: Lagrangian Climatology and Dynamical Impact on the Planetary Boundary Layer, Journal of Climate, 30, 6661 – 6682, https://doi.org/10.1175/JCLI-D-16-0782.1, 2017.

Rixen, M., Pothapakula, P., Sprenger, M., Zeman, C., and Prein, A. F.: Grid-Spacing Sensitivity of Rossby Wave Breaking to Mesoscale Diabatic Processes, EGUsphere, 2026, 1–30, https://doi.org/10.5194/egusphere-2026-1814, 2026.

Rodwell, M. J., Magnusson, L., Bauer, P., Bechtold, P., Bonavita, M., Cardinali, C., Diamantakis, M., Earnshaw, P., Garcia-Mendez, A., Isaksen, L., Källén, E., Klocke, D., Lopez, P., McNally, T., Persson, A., Prates, F., and Wedi, N.: Characteristics of Occasional Poor Medium-Range Weather Forecasts for Europe, Bulletin of the American Meteorological Society, 94, 1393 – 1405, https://doi.org/10.1175/BAMS-D-12-00099.1, 2013.

Schemm, S.: Toward Eliminating the Decades-Old "Too Zonal and Too Equatorward" Storm-Track Bias in Climate Models, Journal of Advances in Modeling Earth Systems, 15, e2022MS003 482, https://doi.org/https://doi.org/10.1029/2022MS003482, e2022MS003482 2022MS003482, 2023.

Schnyder, F. and Riboldi, J.: Linking Upstream Cold, Continental Air to the Intensity of Marine Cold-Air Outbreaks along the Western Boundary Currents of the North Pacific and North Atlantic: A Lagrangian Analysis, Journal of Climate, 39, 2243 – 2262, https://doi.org/10.1175/JCLI-D-25-0336.1, 2026.

Schultz, D. M., Bracken, W. E., and Bosart, L. F.: Planetary- and Synoptic-Scale Signatures Associated with Central American Cold Surges, Monthly Weather Review, 126, 5 – 27, https://doi.org/10.1175/1520-0493(1998)126<0005:PASSSA>2.0.CO;2, 1998.

Schäfler, A. and Harnisch, F.: Impact of the inflow moisture on the evolution of a warm conveyor belt, Quarterly Journal of the Royal Meteorological Society, 141, 299–310, https://doi.org/https://doi.org/10.1002/qj.2360, 2015.

Sodemann, H.: Beyond Turnover Time: Constraining the Lifetime Distribution of Water Vapor from Simple and Complex Approaches, Journal of the Atmospheric Sciences, 77, 413 – 433, https://doi.org/10.1175/JAS-D-18-0336.1, 2020.

Sodemann, H. and Stohl, A.: Moisture Origin and Meridional Transport in Atmospheric Rivers and Their Association with Multiple Cyclones, Monthly Weather Review, 141, 2850 – 2868, https://doi.org/10.1175/MWR-D-12-00256.1, 2013.

Sodemann, H., Schwierz, C., and Wernli, H.: Interannual variability of Greenland winter precipitation sources: Lagrangian moisture diagnostic and North Atlantic Oscillation influence, Journal of Geophysical Research: Atmospheres, 113, https://doi.org/https://doi.org/10.1029/2007JD008503, 2008.

Sprenger, M. and Wernli, H.: The LAGRANTO Lagrangian analysis tool – version 2.0, Geoscientific Model Development, 8, 2569–2586, https://doi.org/10.5194/gmd-8-2569-2015, 2015.

Sprenger, M., Fragkoulidis, G., Binder, H., Croci-Maspoli, M., Graf, P., Grams, C. M., Knippertz, P., Madonna, E., Schemm, S., Škerlak, B., and Wernli, H.: Global Climatologies of Eulerian and Lagrangian Flow Features based on ERA-Interim, Bulletin of the American Meteorological Society, 98, 1739 – 1748, https://doi.org/10.1175/BAMS-D-15-00299.1, 2017.

https://doi.org/10.5194/egusphere-2026-5486
Preprint. Discussion started: 22 September 2026

Steinfeld, D. and Pfahl, S.: The role of latent heating in atmospheric blocking dynamics: a global climatology, Climate Dynamics, 53, 6159–6180, https://doi.org/10.1007/s00382-019-04919-6, 2019.

Sánchez, C., Methven, J., Gray, S., and Cullen, M.: Linking rapid forecast error growth to diabatic processes, Quarterly Journal of the Royal Meteorological Society, 146, 3548–3569, https://doi.org/https://doi.org/10.1002/qj.3861, 2020.

Tamarin-Brodsky, T. and Harnik, N.: The relation between Rossby wave-breaking events and low-level weather systems, Weather and Climate Dynamics, 5, 87–108, https://doi.org/10.5194/wcd-5-87-2024, 2024.

Tamarin-Brodsky, T. and Kaspi, Y.: Enhanced poleward propagation of storms under climate change, Nature Geoscience, 10, 908–913, https://doi.org/10.1038/s41561-017-0001-8, 2017.

Tamarin-Brodsky, T., Harnik, N., and Falkena, S. K. J.: On Storm Tracks, Weather Regimes, and a Wave Breaking Recipe, AGU Advances, 7, e2025AV002 049, https://doi.org/https://doi.org/10.1029/2025AV002049, e2025AV002049 2025AV002049, 2026.

Walker, C. C. and Schneider, T.: Eddy Influences on Hadley Circulations: Simulations with an Idealized GCM, Journal of the Atmospheric Sciences, 63, 3333 – 3350, https://doi.org/10.1175/JAS3821.1, 2006.

Walsh, J. E., Phillips, A. S., Portis, D. H., and Chapman, W. L.: Extreme Cold Outbreaks in the United States and Europe, 1948–99, Journal of Climate, 14, 2642 – 2658, https://doi.org/10.1175/1520-0442(2001)014<2642:ECOITU>2.0.CO;2, 2001.

Wenta, M., Grams, C. M., Papritz, L., and Federer, M.: Linking Gulf Stream air–sea interactions to the exceptional blocking episode in February 2019: a Lagrangian perspective, Weather and Climate Dynamics, 5, 181–209, https://doi.org/10.5194/wcd-5-181-2024, 2024.

Wernli, H. and Davies, H. C.: A Lagrangian-based analysis of extratropical cyclones. I: The method and some applications, Quarterly Journal of the Royal Meteorological Society, 123, 467–489, https://doi.org/https://doi.org/10.1002/qj.49712353811, 1997.

Wernli, H. and Gray, S. L.: The importance of diabatic processes for the dynamics of synoptic-scale extratropical weather systems – a review, Weather and Climate Dynamics, 5, 1299–1408, https://doi.org/10.5194/wcd-5-1299-2024, 2024.

Wernli, H. and Schwierz, C.: Surface Cyclones in the ERA-40 Dataset (1958–2001). Part I: Novel Identification Method and Global Climatology, Journal of the Atmospheric Sciences, 63, 2486 – 2507, https://doi.org/10.1175/JAS3766.1, 2006.

Yamamoto, A., Nonaka, M., Martineau, P., Yamazaki, A., Kwon, Y.-O., Nakamura, H., and Taguchi, B.: Oceanic moisture sources contributing to wintertime Euro-Atlantic blocking, Weather and Climate Dynamics, 2, 819–840, https://doi.org/10.5194/wcd-2-819-2021, 2021.

Yu, Q., Spensberger, C., Magnusson, L., and Spengler, T.: Forecast Errors Attributed to Synoptic Features, Meteorological Applications, 32, e70 093, https://doi.org/https://doi.org/10.1002/met.70093, e70093 MET-25-0059.R1, 2025.